ISSN 1054-660X, Laser Physics, 2010, Vol. 20, No. 1, pp. 47–51.

PAPERS

Atomic Diffraction Microscope of the de Broglie Waves

V. I. Balykin

Institute of Spectroscopy, Troitsk, Moscow region, Russia

Institute of Laser Sciences, University of Electro-Communications, Tokyo, Japan

Received February 15, 2009

Abstract—We consider a new approach to the atomic microscopy of the de Broglie waves based on the diffraction rather than refraction phenomenon. It is demonstrated that a diffraction objective that images an object with a magnification of 10^3 can be implemented at appropriate parameters of the atomic-wave diffraction by a circular aperture in a real screen.

DOI: 10.1134/S1054660X09180030

1. INTRODUCTION

All of the known types of wave microscopy are based on the wave refraction in the presence of an external potential (the wave reflection is a particular case of the wave refraction by a potential whose characteristic size is less than the corresponding wavelength). A specific implementation of a microscope depends on the technical implementation of the refractive medium: transparent (at the given wavelength) materials serve as refracting media for electromagnetic fields and electromagnetic fields with the corresponding configurations work as refracting media for the waves of material particles (electrons and ions). The advent of atom optics [1–3] has stimulated a search for the microscopic methods using neutral atoms [4]. The microscopy based on the application of neutral atoms has several significant advantages in comparison with the electron and ion microscopy [5]. Both electron and ion microscopes have an atomic resolution of about 1 Å but electrons and ions can easily damage the object under study due to a relatively high (about 100 keV) energy of the particles. In addition, the object can be charged by the electron (ion) beam and, hence, the image can be distorted. A microscope based on neutral atoms can perfectly combine a relatively low kinetic energy (nondestructive probing) and a relatively small de Broglie wavelength (high resolution).

Various configurations of electromagnetic fields serve as refracting media in atomic optics (as well as in electron (ion) optics) [4–11]. The main problems in the practical atomic microscopy are as follows: (i) the difficulties in the generation of potentials for the atomic interaction with electromagnetic field that allow the sharp focusing of the atomic beam close to the diffraction limit and (ii) relatively weak interaction forces on neutral atoms from the known fields which necessitate the application of cold atomic beams that exhibit a relatively large de Broglie wavelength and, hence, a relatively large limiting size of the focusing spot. In this work, we consider an alternative approach to the atomic microscopy based on the atomic diffraction rather than the atomic refraction. Normally, the wave diffraction is a limiting factor for any wave microscopy. However, we will demonstrate a possibility of the atomic microscopy based on the diffraction phenomenon and the recent progress in nanotechnology.

2. PHYSICS AND MATHEMATICS OF THE DIFFRACTION MICROSCOPE

The phenomenon of diffraction was intensively investigated in atom optics [2, 3] and it was convincingly experimentally proved of the validity of laws of wave mechanics also in relation to complex multipartial quantum objects such as neutral atoms [12–14]. In this work, the main principle of the atomic focusing and the construction of the corresponding atomic microscopy is based on the boundary diffraction wave. The notion of the boundary diffraction wave was introduced for the physical interpretation and, then, the mathematical analysis of the wave diffraction. When a wave is incident on the screen with a hole, the wave distribution behind the screen can be considered as a result of the interference of the incident wave and the wave scattered by the edges of the hole (the boundary diffraction wave). The concept of the diffraction resulting from the interference of such waves was proposed by Young who preceded Fresnel in an attempt to theoretically interpret the diffraction using the wave theory. Several authors employed this approach in the analysis of diffraction (see the corresponding references in M. Born and E. Wolf, *Principles of Optics* (1964)).

Figure 1 shows the scheme for atom focusing based on wave diffraction. A wave emitted at point S is incident on the screen with a circular aperture of radius a. We consider the wave-intensity distribution behind the screen at point P. The optics of material particles and the conventional optics employ the same mathemati-

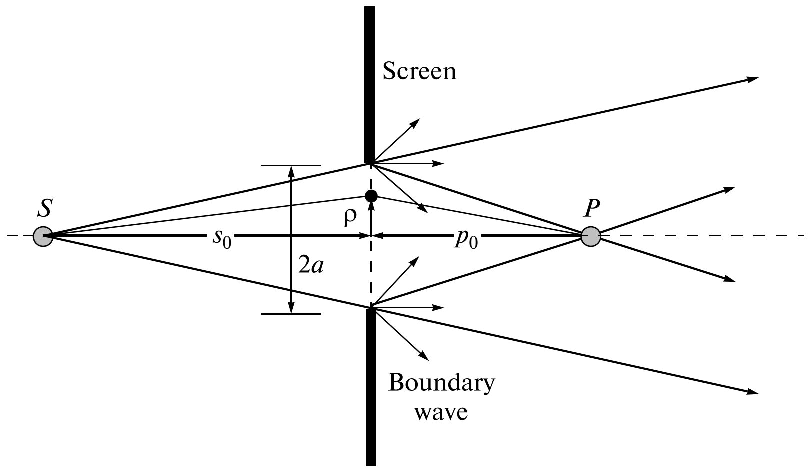

Fig. 1. Schematic drawing that shows image P of point source S resulting from the interference of the incident wave and the boundary diffraction wave in the presence of a screen.

cal apparatus. Thus, we analyze the diffraction of atomic waves using the optical diffraction theory taking into account the corresponding refractive indices (for both photons and atoms). The field-amplitude distribution at point P at the axis of the system is given by the Rayleigh integral [15, 16]

$$U(p) = -p_0\int_0^a \frac{\exp(ikr_s)}{r_s}\frac{1}{r_p}\frac{1}{\partial r_p}\left(\frac{\exp(ikr_s)}{r_s}\right)\rho d\rho, \quad (1)$$

where $r_s = (s_0^2+\rho^2)^{1/2}$, $r_p = (p_0^2+\rho^2)^{1/2}$, s_0 is the distance from the source to the screen, p_0 is the distance from the screen to the image plane, and ρ is the transverse coordinate in the aperture plane.

Using expression (1), we can derive an analytical expression for the wave-field distribution [15, 16]:

$$U(p) = \exp[ik(s_0+p_0)]/(s_0+p_0) + \cos\alpha\exp(i\pi)\exp(ikp)/p, \quad (2)$$

where $p = (s_0^2+a^2)^{1/2} + (p_0^2+a^2)^{1/2}$, $\cos\alpha = p_0/(p_0^2+a^2)^{1/2}$, $k = 2\pi/\lambda$, and λ is the wavelength.

The physical interpretation of result (2) for the wave amplitude behind the screen at point P is as follows. The first term in expression (2) corresponds to the contribution of the spherical wave emitted by the source at point S to field-amplitude distribution. The second term describes the contribution of the spherical wave that propagates from source S to the edge of the aperture and from the edge of the aperture to observation point P (this contribution corresponds to the boundary diffraction wave). The amplitude of the wave scattered by the edge of the aperture is $\cos\alpha$. The amplitude ratio of the two waves equals

$$\eta \cong \left(1 - \frac{a^2}{2s_0^2} - \frac{a^2}{2s_0p_0}\right). \quad (3)$$

If the aperture size satisfies the inequalities $a \ll s_0, p_0$ and $a \gg \lambda$, the contributions of the boundary diffraction wave and the wave incident on the screen can be on the same order of magnitude. It follows from expression (2) that the wave intensity at point P is given by

$$U^2(p) = \frac{1}{(s_0+p_0)^2}\left\{1 - 2\cos\alpha\left(\frac{s_0+p_0}{p}\right)\cos[k(\Delta+\Delta_0)] + \cos^2\alpha\frac{(s_0+p_0)^2}{p^2}\right]. \quad (4)$$

If the source–screen distance is significantly greater than the aperture size ($s_0 \gg a$), expression (4) can be represented as

$$U^2(p_0) = \frac{1}{(s_0+p_0)^2}\{2 - 2\cos[(\Delta+\Delta_0)k]\}. \quad (5)$$

We define the focal point of the diffraction objective as the axial point with the maximum intensity. Then, in accordance with expression (5), the focal length of the diffraction objective is determined from the condition $\cos[k(\Delta+\Delta_0)] = -1$. Thus, the lens formula of the diffraction objective is written as

$$\frac{1}{s_0} + \frac{1}{p_0} = \frac{1}{(a^2/m\lambda)}, \quad m = 1, 3, 5, \ldots \quad (6)$$

and the focal length is given by

$$f = a^2/m\lambda. \quad (7)$$

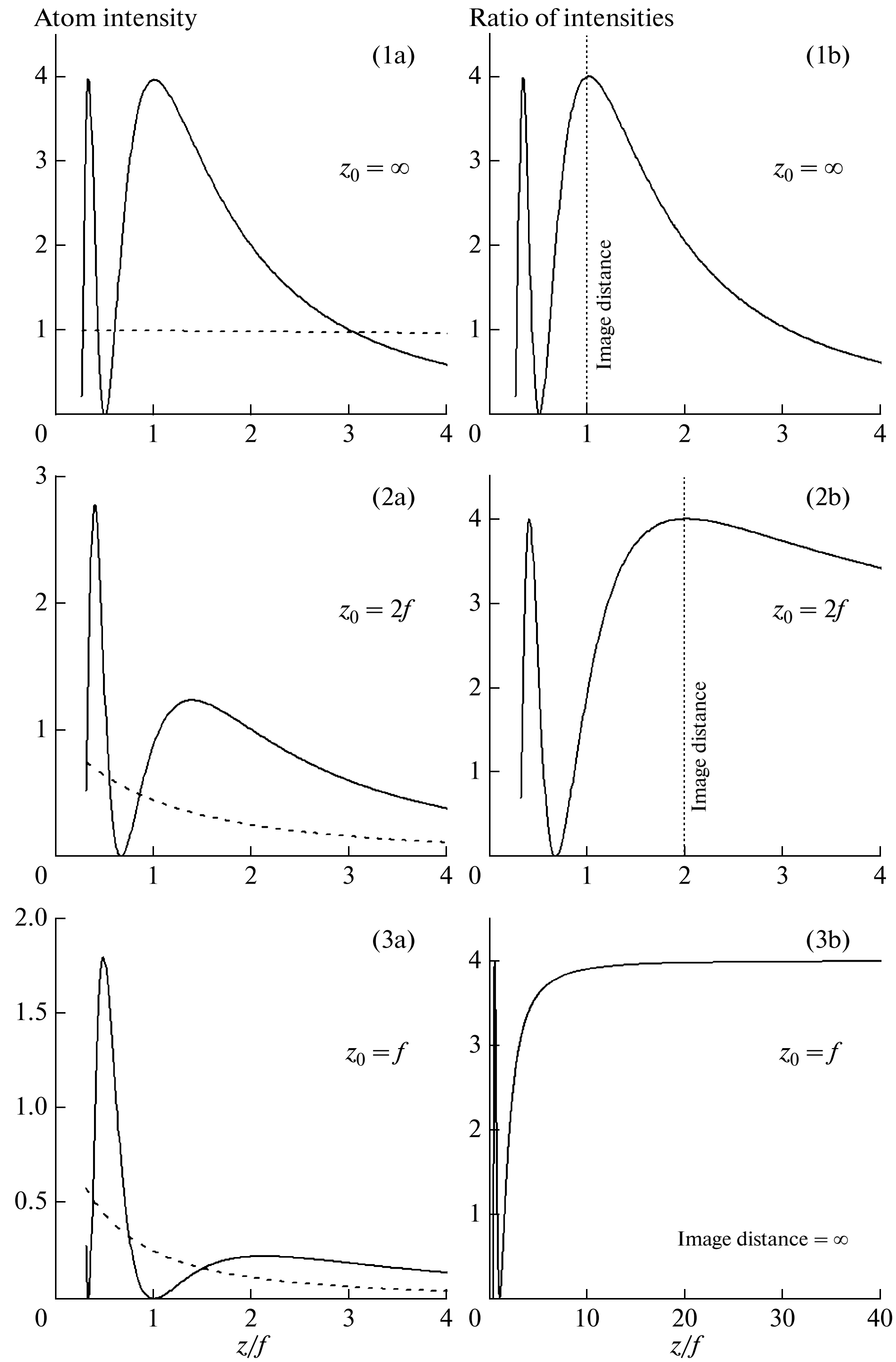

Fig. 2. Plots of (a) the axial intensity of the wave having passed through the diffraction objective and (b) the intensity ratio of the wave at the axis of the diffraction objective and the wave in the absence of the screen vs. the distance from the objective for (1) the infinite distance between the source and the screen, (2) $p_0 = 2f$, and (3) $p_0 = f$. The dashed lines in panels (a) and (b) show the axial intensities in the absence of the screen and the positions of the image plane of the diffraction objective, respectively.

Formula (5) shows that an increase in the wave intensity at the axis of the diffraction objective is represented as

$$\xi = \{2 - 2\cos[k(\Delta_0 + \Delta)]\}. \quad (8)$$

The maximum increase is $\xi_{max} = 4$.

3. MAIN CHARACTERISTICS

Figure 2 illustrates the focusing by the diffraction objective. The solid lines in panels (1a)–(3a) show the curves of the wave intensity at the axis of the diffraction objective versus the distance between the screen and the image plane. The dashed line corresponds to the wave intensity at the axis in the absence of the

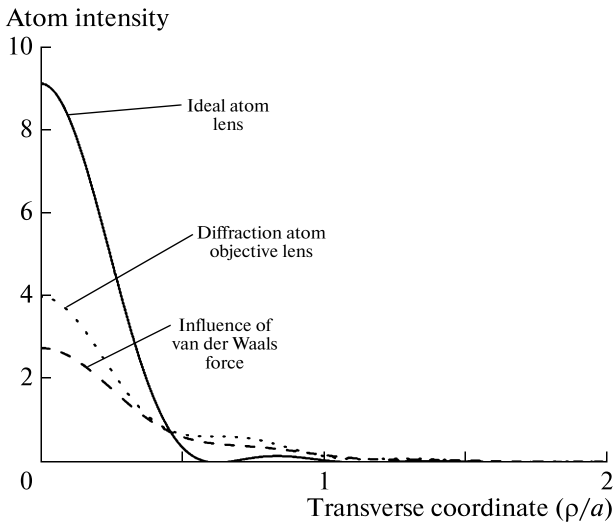

Fig. 3. Transverse distributions of the intensity of the atomic de Broglie wave at the focal plane of the diffraction objective for a perfect objective, a perfect diffraction objective, and a real diffraction objective.

screen. Panels (1b)–(3b) demonstrate the ratios of the two intensities. The curves are obtained using the data from the left-hand panels and illustrate the focusing by the diffraction objective. In the calculations, we employ the de Broglie wavelength $\lambda_B = 0.1$ nm and the aperture radius $a = 25$ nm. The distance from the screen is measured in the units of the principal focal length $f = a^2/\lambda$, which is 6.2 μm for the above parameters. Panels (1a) and (1b) in Fig. 2 correspond to the wave source located at the infinite distance (a plane wave is incident on the screen). Panel (1b) shows the wave focusing at the distance $z = f$ in accordance with formula (6).

Panels (2a) and (2b) in Fig. 2 correspond to the source located at a distance of two focal lengths from the screen ($s_0 = 2f$). Formula (6) predicts the maximum wave intensity at the distance $z = 2f$ behind the screen. The results of the exact calculation based on diffraction integral (1) (panel (2b) in Fig. 2) provides the supporting evidence: the intensity maximum corresponds to two focal lengths. When the source is located at the distance equal to the focal length ($s_0 = f$) (panels (3a) and (3b) in Fig. 2), the wave behavior behind the screen is similar to the wave behavior in a system with a conventional optical lens: the image of the source located at the focal length is formed at an infinite distance. Note that, in this case, the intensity ratio at large distances ($p_0 > 10f$) takes on a constant value of 4 (panel (3b) in Fig. 2).

The resolution of the diffraction objective can be studied using the Fresnel diffraction theory. We consider a plane wave incident on the screen with an aperture and we search for the transverse wave-amplitude distribution at the distance equal to the focal length (panels (3a) and (3b) in Fig. 2). The amplitude distribution is determined by the Fresnel diffraction integral [17]:

$$U(x_f, y_f) = \frac{1}{i\lambda f}\exp\left[i\frac{k}{f}(x_f^2 + y_f^2)\right. \times \left.\int_{x,y} W(x, y)\exp\left[-i\frac{k}{f}(xx_f + yy_f)\right]dxdy\right], \quad (9)$$

where (x_f, y_f) are the transverse coordinates in the focal plane, $k = 2\pi/\lambda$, and $W(x, y)$ is the amplitude–phase transparency (APT) at the aperture in the screen.

For the idealized case of the wave diffraction by an aperture in an infinitely thin screen, the APT is

$$W(x, y) \equiv 1. \quad (9.1)$$

When the aperture is changed by a perfect lens, the APT is given by

$$W(x, y) = \exp\left[-i\frac{k}{2f}(x^2 + y^2)\right]. \quad (9.2)$$

For a real physical aperture in a material screen, the APT for the de Broglie waves is represented as

$$W(x, y) = \exp[-i\varphi(x, y)], \quad (9.3)$$

where $\varphi(x, y)$ is the phase shift of the wave due to the van der Waals potential of the screen walls. With allowance for the short-range repulsive potential, the van der Waals potential is simulated using the function

$$V(\rho) = A\exp[-\alpha(a-\rho)] - c_3/(a-\rho)^3, \quad (10)$$

where the first term corresponds to the repulsive surface potential and the second term determines the attractive van der Waals potential. Coefficients A, α, and c_3 are the characteristic parameters of the potentials. We consider the silicon-nitride screen with the thickness $h = 50$ nm, the aperture radius $a = 25$ nm, and the metastable He atoms with the de Broglie wavelength $\lambda_B = 0.1$ nm. The parameters of the potentials are [18] $A = 4 \times 10^{13}$ Hz, $\alpha = 2 \times 10^9$ m^{-1}, and $c_3 = 1.8 \times 10^{-50}$ J m^3.

Figure 3 shows the transverse intensity distribution of the de Broglie wave at the focal plane for (a) a perfect objective whose APT is given by expression (9.2), (b) a perfect diffraction objective whose APT is given by expression (9.1), and (c) a real diffraction objective whose APT is given by expression (9.3). The comparison shows that the axial intensity of the wave for the perfect objective is greater than the intensities for the perfect and real diffraction objectives by factors of 2 and 2.5, respectively. The FWHMs of the distributions are comparable and are close to the diffraction value, which is $\rho = 7$ nm for the given configuration. For the real diffraction objectives, the atoms are partially scattered by near-wall potential (10) and this effect contributes to the wings of the distribution. Thus, a real diffraction objective with the appropriate parameters can be close to a perfect objective with respect to the focusing.

4. SCHEME OF THE ATOMIC DIFFRACTION MICROSCOPE

The scheme of the atomic microscope based on the diffraction objective can be similar to the scheme of the conventional optical or electron microscope. When an object is located at a distance close to or greater than the focal length ($f = 6.2$ μm), we can easily reach a magnification of 10^3 at the distance z = 0.6 mm from the screen. When the size of an atomic object equals the minimum spot size in the focal plane (Fig. 3), the image size (7 μm) is comparable with the pixel size of the multichannel plate that is used for detection of metastable ions (*He and *Ne).

Note that a zone plate (a well-known element in various types of wave optics) also employs the diffraction for the wave focusing. However, the zone plate can hardly be used for imaging [19], since is represents an aperiodic diffraction grating that concentrates a significant part of the intensity of the incident wave in a large number of high-order diffraction peaks.

5. CONCLUSIONS

New approach to a problem of the atomic microscopy based on atomic diffraction rather than the atomic refraction is considered. Diffraction of atomic wave, as a rule, is the fundamental limiting factor of any wave microscopy. However, as has been shown, on the basis of this phenomenon and using the last achievement in nanotechnology, it is possible to create a new type of microscopy of atomic de Broglie waves.

ACKNOWLEDGMENTS

This work was supported in part the Russian Foundation for Basic Research (project nos. 08-02-00653a, 08-02-00871a, and 09-02-01022a). I am grateful to F. Shimizu, V.S. Letokhov, V.G. Minogin, P.N. Melent’ev, and A.E. Afanas’ev for helpful discussions.

REFERENCES

1. V. I. Balykin and V. S. Letokhov, Phys. Today **4**, 23 (1989).
2. C. S. Adams, M. Sigel, and J. Mlynek, Phys. Rep. **240**, 141 (1994).
3. P. Meystre, *Atom Optics* (Springer New York, 2001).
4. V. I. Balykin and V. S. Letokhov, Zh. Eksp. Teor. Fiz. **94**, 140 (1988); V. I. Balykin and V. S. Letokhov, Opt. Commun. **64**, 151 (1987).
5. Appl. Phys. B **54**, Spec. Issue *Optics and Interferometry with Atoms*, Ed. by J. Mlynek, V. I. Balykin, and P. Meystre (1992).
6. J. J. McClelland, R. E. Sholten, E. C. Palm, and R. J. Celotta, Science **262**, 877 (1993).
7. V. I. Balykin, V. S. Letokhov, and V. V. Klimov, Pis’ma Zh. Eksp. Teor. Fiz. **59**, 219 (1994) [JETP Lett. **59**, 235 (1994)].
8. H.-R. Noh, K. Shimizu, and F. Shimizu, Phys. Rev. A **61**, 041601 (2000).
9. V. I. Balykin, V. S. Letokhov, and V. V. Klimov, Pis’ma Zh. Eksp. Teor. Fiz. **78**, 8 (2003) [JETP Lett. **78**, 8 (2003)].
10. V. I. Balykin and V. G. Minogin, Phys. Rev. A **77**, 01360 (2008).
11. D. Kouznetsov, H. Oberst, A. Neumann, Y. Kuznetsova, K. Shimizu, J.-F. Bisson, K. Ueda, and S. R. J. Brueck, J. Phys. B: At. Mol. Opt. Phys. **39**, 1605 (2006).
12. D. W. Keith, M. L. Schattenburg, H. I. Smith, and D. E. Pritchard, Phys. Rev. Lett. **61**, 1580–1583 (1988).
13. O. Carnal and J. Mlynek, Phys. Rev. Lett. **66**, 2689 (1991).
14. E. M. Rasel, M. K. Oberthaler, H. Batelaan, J. Schmiedmayer, and A. Zeilinger, Phys. Rev. Lett. **75**, 2633 (1995).
15. C. J. Bouwkamp, Rep. Prog. Phys. **17**, 39 (1954).
16. H. Osterberg and L. W. Smith, JOSA **51**, 1050 (1961).
17. J. W. Goodman, *Introduction to Fourier Optics* (McGraw-Hill, New York, 1968).
18. R. E. Grisenti, W. Schöllkopf, J. P. Toennies, G. C. Hegerfeldt, and T. Köhler, Phys. Rev. Lett. **83**, 1755 (1999).
19. M. Bottema, JOSA **59**, 1632 (1969).